

# Mid-infrared Sensors with InAs/GaSb Superlattice Absorption Layers Grown on InP Substrates

Kohei MIURA\*, Yasuhiro IGUCHI, Tsukuru KATSUYAMA and Yuichi KAWAMURA

Type-II InAs/GaSb superlattices (SLs), which are attractive for the absorption layers of mid-infrared sensors, are usually grown on GaSb substrates. However, since GaSb substrates absorb infrared light, other substrates with high transparency are favorable for back-illuminated sensors. We have focused on InP substrates with high transparency and relatively small lattice mismatch to GaSb. The crystallographic and optical properties of SLs have been improved as the GaSb buffer layer thickness increases due to the reduction of threading dislocations. We have successfully fabricated sensors with the cutoff wavelength of 6.5  $\mu\text{m}$  using InAs/GaSb SL absorption layers grown on InP substrates for the first time.

Keywords: GaSb, InAs, type-II superlattice, InP, mid-infrared sensor

## 1. Introduction

Mid-infrared sensors with the cutoff wavelength over 3  $\mu\text{m}$  utilizing HgCdTe absorption layers are widely used for gas sensing, thermal detection, and so on. Recently, type-II InAs/GaSb superlattices (SLs) are regarded as promising alternative material systems. The band structure of InAs/GaSb SL is shown in **Fig. 1**. The bottom of the conduction band of InAs is lower than that of GaSb, and the top of the valence band of GaSb is higher than that of InAs. SLs with such band structure are called type-II. Long cutoff wavelength can be achieved due to the formation of minibands of electrons and holes<sup>(1)</sup>. Lower dark current is expected from InAs/GaSb SLs compared to HgCdTe because of the higher effective masses of carriers and suppressed Auger recombination<sup>(2)</sup>. Moreover, the cutoff wavelength can be controlled easily by changing the thicknesses of InAs and GaSb layers<sup>(3)</sup>.

Among mid-infrared sensors, focal plane arrays (FPAs) are attractive. Recently, many researchers have been reported FPAs with InAs/GaSb SL absorption layers<sup>(4)-(6)</sup>. However, there are several problems. FPAs consist of sensor chips and read-out integrated circuits (ROICs) bonded to each other via bump metals. Sensor chips are made of epitaxial wafers, usually grown on GaSb substrates. Unfortunately, in the case of back-illuminated sensors such as FPAs, the large absorption coefficients of GaSb substrates

in the infrared region decrease the sensitivities of the sensors<sup>(7)</sup>. Furthermore, the large difference in the thermal expansion coefficient between GaSb and silicon deteriorates the reliability of the FPA, since the ROICs are made of silicon. When the FPA is cooled down to an operational temperature lower than 100 K, significant stress is applied to the bonded parts due to the difference in the thermal expansion coefficient. To avoid these problems, the GaSb substrates should be thinned or nearly removed, by using difficult techniques<sup>(8),(9)</sup>. The InAs/GaSb SLs grown on GaAs substrates with higher transparency in the infrared region are proposed and demonstrated<sup>(7)</sup>. However, the GaAs has the problem that the large lattice mismatch between GaAs and GaSb (7.8%) makes the epitaxial growth difficult<sup>(10),(11)</sup>. In addition, the difference in the thermal expansion coefficient between GaAs and silicon is large.

The authors have focused on InP substrates not only because of high transparency in the mid-infrared region but also due to a smaller lattice mismatch to the GaSb as listed in **Table 1 (a)**. Moreover, InP has a thermal expansion coefficient which is closer to that of Si than GaAs and GaSb (**Table 1 (b)**). In this study, we report on successful growth of type-II InAs/GaSb SLs on InP substrates and fabrication of mid-infrared sensors using the SLs.

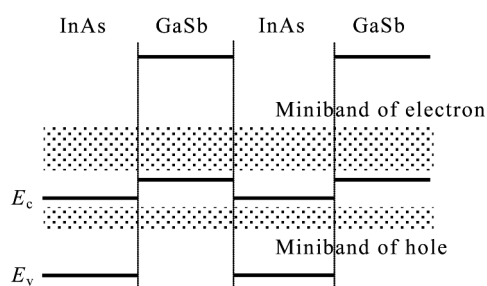


**Fig. 1.** Band structure of InAs/GaSb SL

**Table 1.** Parameters of GaSb, GaAs, InP

(a) Lattice constant			
	Lattice constant (Å)	Lattice mismatch with GaSb	Ref.
GaSb	6.096	-	[12]
GaAs	5.653	7.8%	[12]
InP	5.870	3.9%	[12]

(b) Thermal expansion coefficient		
	Thermal expansion coefficient ( $10^{-6} \text{ K}^{-1}$ )	Ref.
Si	3.34	[13]
GaSb	7.74	[12]
GaAs	6.86	[12]
InP	4.75	[12]

## 2. Experimental Details

First of all, the absorption coefficient of InP substrates was measured. Absorption coefficient spectra of several substrates are shown in **Fig. 2**. An Fe-doped InP substrate was proved to have a lower absorption coefficient in the wavelength range of 3-12  $\mu\text{m}$  compared to an un-doped GaSb substrate and a Te-doped GaSb substrate, probably due to less free carrier absorption. In this study, we used Fe-doped InP substrates.

Epitaxial growths are performed by solid source molecular beam epitaxy (MBE) method. In and Ga metals are used as group III beam sources and supplied by conventional effusion cells. Group V sources of As and Sb are supplied by needle-valve cracking cells. The cracking temperatures are kept at 600°C and 800°C for As and Sb, respectively.

Epitaxial layers with three kinds of structures were grown. The first is a GaSb single layer. GaSb buffer layers are used for the growth of InAs/GaSb SLs on InP substrates. We have studied the influence of lattice mismatch between InP and GaSb on the crystallographic property of GaSb. Prior to the growth, the Fe-doped (100) InP substrate surface was cleaned under As vapor pressure<sup>(14)</sup>. 0.15  $\mu\text{m}$ -thick  $\text{In}_{0.53}\text{Ga}_{0.47}\text{As}$  layers were grown in order to smoothen the surfaces of the substrates. Subsequently, GaSb buffer layers were grown.

The second is an InAs/GaSb SL. After growing  $\text{In}_{0.53}\text{Ga}_{0.47}\text{As}$  layers and GaSb buffer layers by the same procedure mentioned above, type-II InAs/GaSb SLs, which consist of 50 pairs of 3.5 nm-thick InAs and 2.1 nm-thick GaSb, were grown. The growth rates of GaSb and InAs were both 0.55  $\mu\text{m}/\text{h}$ . An SL on a GaSb substrate was also grown using a 0.15  $\mu\text{m}$ -thick GaSb buffer layer as a reference. The SL has the same periodic structure with the SLs on InP substrates.

The third is an epitaxial wafer for sensor fabrication. A type-II InAs/GaSb SL, which consists of 100 pairs of 3.6 nm-thick InAs and 2.1 nm-thick GaSb, was grown on the InP substrate by the same procedure described above. A GaSb buffer layer with the thickness of 4.5  $\mu\text{m}$  was used because a thick GaSb buffer layer is effective in improving the crystallographic property of the SL as described in the next chapter. In order to obtain p-i-n structure, the GaSb buffer

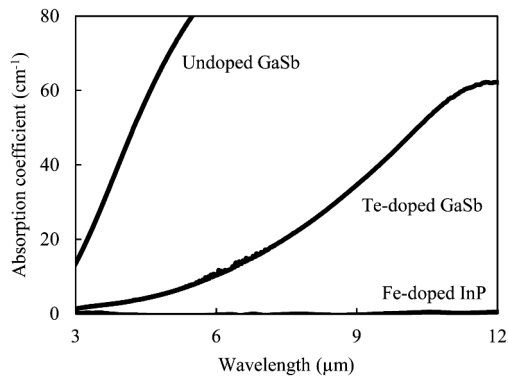


**Fig. 2.** Absorption coefficient spectra of InP and GaSb substrates

layer was doped by Be as an acceptor. The GaSb layers in the bottom 30 pairs of SL were also doped by Be. The InAs layers in the upper 30 pairs of SL were doped by Si as a donor. The middle 40 pairs were not intentionally doped. Finally, an Si-doped InAs cap layer with the thickness of 20 nm was grown on the SLs. As a reference, an InAs/GaSb SL was grown on a Te-doped (100) GaSb substrate, where Be-doped GaSb buffer layers with the thickness of 0.5  $\mu\text{m}$  and Si-doped InAs cap layers with the thickness of 20 nm were also grown.

The crystallographic properties of the epitaxial wafers were characterized by optical microscope, X-ray diffraction with  $\text{Cu K}\alpha_1$  ( $\lambda = 1.54056 \text{ \AA}$ ), cross sectional transmission electron microscopy (TEM), and photoluminescence (PL) with a YAG laser (1064 nm) and an HgCdTe detector.

The structure of the mid-infrared sensor is illustrated in **Fig. 3**. The circle mesa structures were formed by wet chemical etching. The mesa diameters were varied from 30 to 920  $\mu\text{m}$ . SiN layers were used for etching masks. A solution, including phosphoric acid ( $\text{H}_3\text{PO}_4$ ), citric acid ( $\text{C}_6\text{H}_8\text{O}_7$ ), hydrogen peroxide ( $\text{H}_2\text{O}_2$ ) and water ( $\text{H}_2\text{O}$ ), was used for etchant. The sidewalls of the mesa structures were passivated by an  $\text{SiO}_2$  deposited using a plasma-enhanced chemical vapor deposition. Ti/Pt/Au electrodes were evaporated on both Si-doped InAs cap layers and Be-doped GaSb buffer layers which were revealed by mesa-etching. Sensors on the GaSb substrates were also fabricated simultaneously.

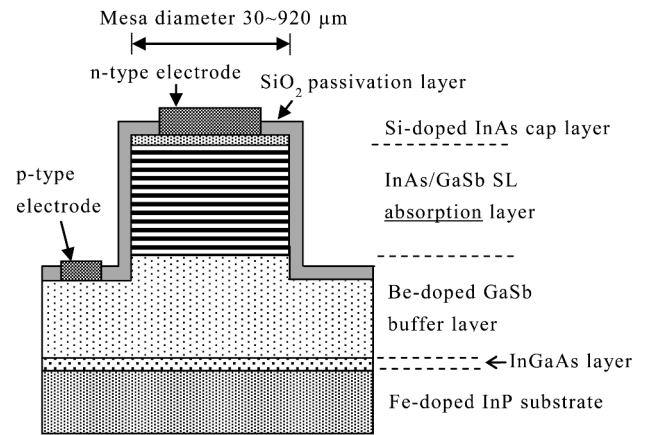


**Fig. 3.** Structure of the sensor on the InP substrate

## 3. Results and Discussion

### 3-1 GaSb single layers on InP substrate

Two GaSb layers with different thicknesses were grown; 0.5  $\mu\text{m}$  and 2  $\mu\text{m}$ . The X-ray rocking curves (XRCs) are shown in **Fig. 4**. The diffraction peaks of GaSb (400) are broad but single. Calculated diffraction peak positions of fully-relaxed GaSb and GaSb without relaxation (“not-relaxed” in **Fig. 4**) are also shown as dotted lines. The GaSb layers are inferred to be almost fully-relaxed from the peak

positions. However, no crosshatches are observed on the surfaces (Fig. 5). The thicker GaSb showed a diffraction peak with narrower full width half maximum (FWHM), indicating crystalline quality is improved by growing thicker layer.

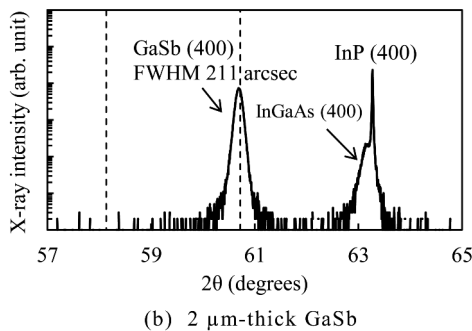
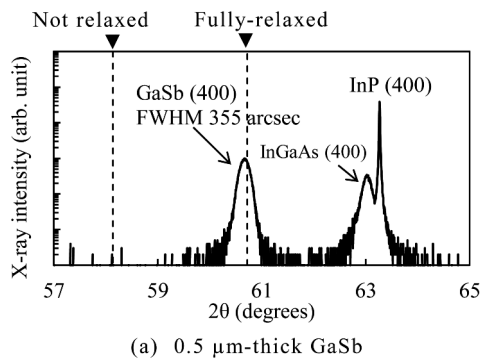


Fig. 4. XRCs of GaSb single layers on InP substrates

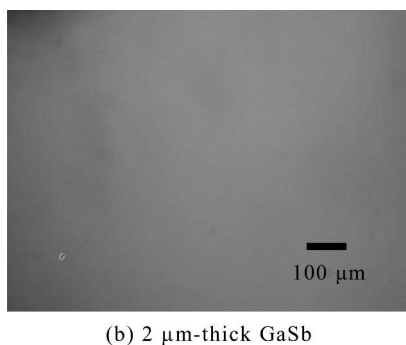
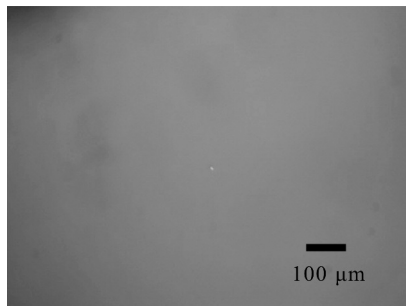


Fig. 5. Surfaces of GaSb single layers on InP substrates observed by optical microscopy

### 3-2 InAs/GaSb SLs on InP substrate

InAs/GaSb SLs were grown on InP substrates using GaSb buffer layers with different thicknesses. The XRCs of the SLs are shown in Fig. 6. In both XRCs, the peak positions of the SLs seem to coincide with those of GaSb buffer layers, probably due to the incorporation of Sb in the InAs layers. Clear satellite peaks are seen, indicating that periodic structures are formed. From the results of fitting, the periods of the SLs on a 0.5  $\mu\text{m}$ -thick buffer layer and a 2.5  $\mu\text{m}$ -thick buffer layer are proved to be 5.60 nm and 5.72 nm, respectively. The SL on a 2.5  $\mu\text{m}$ -thick buffer layer exhibits narrower satellite peaks than the SL on a 0.5  $\mu\text{m}$ -thick buffer layer. The FWHM of the +1st satellite peaks of the SLs on a 0.5  $\mu\text{m}$ -thick buffer layer and a 2.5  $\mu\text{m}$ -thick buffer layer are 344 arc-sec and 175 arc-sec, respectively. The crystallographic property of the SL seems to be improved by increasing GaSb buffer layer thickness.

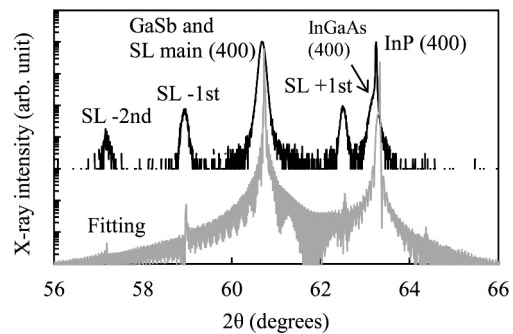
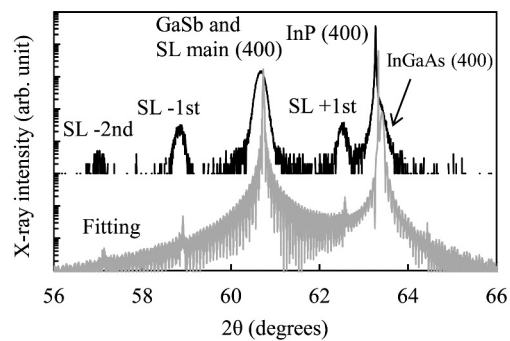
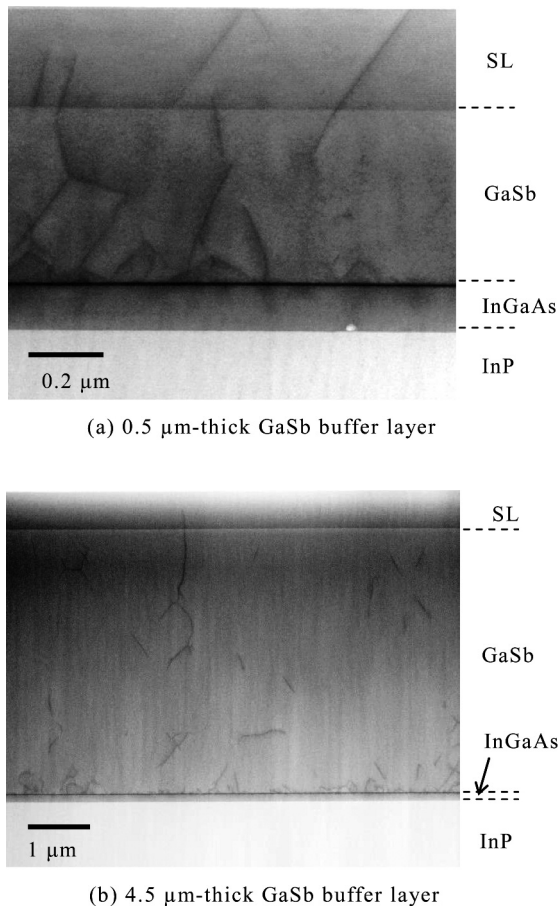


Fig. 6. XRCs of SLs grown on InP substrates

Cross sectional images of the SLs have been observed by TEM. Five threading dislocations are clearly seen in the region of 0.8  $\mu\text{m}$  wide in the SL on a 0.5  $\mu\text{m}$ -thick buffer layer (Fig. 7 (a)). The linear density of the threading dislocations is approximately  $6.3 \times 10^4 \text{ cm}^{-1}$ . The dislocations generated at the initial stage of GaSb growth propagate to the SL. The dislocations in the upper region of the GaSb buffer layer are reduced, suggesting that the threading dislocations annihilated one another as the growth proceeded, similar to GaSb grown on GaAs<sup>(11)</sup>. TEM observations of an SL on a 4.5  $\mu\text{m}$ -thick GaSb buffer layer have been per-

formed on several positions. One of the TEM images is shown in **Fig. 7 (b)**. The linear density of the threading dislocations is  $5.0 \times 10^2 \text{ cm}^{-1}$ , which is lower by two orders of magnitude than that in the SL on a 0.5  $\mu\text{m}$ -thick buffer layer. Thick GaSb buffer layers are preferable for growth of SLs because threading dislocations decrease during buffer layer growth, resulting in fewer dislocations propagating to SL. This result agrees with the FWHMs of X-ray diffraction peaks of GaSb layers.



**Fig. 7.** Cross sectional TEM images of SLs grown on InP substrates

PL measurements have been performed on the SLs on the InP substrates with 0.5  $\mu\text{m}$ -thick and 2.5  $\mu\text{m}$ -thick GaSb buffer layers at 4 K (**Fig. 8**). The SL grown on a GaSb substrate has been also characterized. PL peaks are observed at wavelengths around 6.5  $\mu\text{m}$ . The fluctuation of the PL wavelengths seems to be derived from fluctuation of the SL periods. Both SLs on the InP substrates show stronger PL peak intensities than the SL on the GaSb substrate. In particular, the SL on a 2.5  $\mu\text{m}$ -thick GaSb buffer layer shows PL peak intensity approximately three times stronger than that of the SL on a 0.5  $\mu\text{m}$ -thick buffer layer. The reason why the PL intensities of SLs on InP substrates are stronger than that of the SL on GaSb substrate is not known yet. However, it can be said that SLs with high optical quality are obtained on InP substrates.

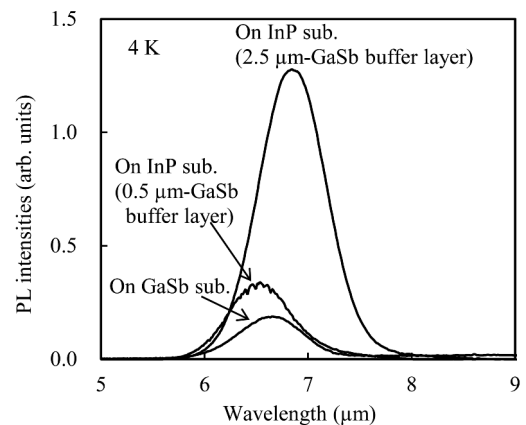


**Fig. 8.** PL spectra of InAs/GaSb SL

### 3-3 Sensors on InP substrate

Current-voltage characteristics of the sensors on the InP substrate and the GaSb substrate at several temperatures (205 K, 145 K and 112 K) are shown in **Fig. 9**. The low current densities of the sensor on the GaSb substrate at forward bias seem to be derived from the high device resistance due to the thin Be-doped GaSb buffer layer. At reverse bias, the dark current of the sensor on the InP substrate is comparable to that on the GaSb substrate at 205 K. However, the separation of the dark current densities becomes more noticeable at lower temperatures. The ideal factor of the sensor on the InP substrate calculated from the current-voltage characteristics at 112 K is 1.7, which indicates that the current of the sensor on the InP

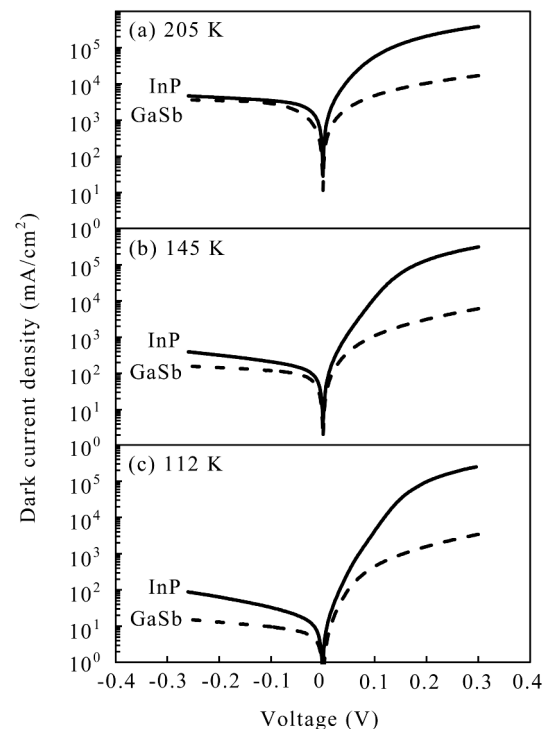


**Fig. 9.** Current-voltage characteristics of the sensors on InP and GaSb substrates

substrate is mainly composed of generation-recombination current rather than diffusion current. It is inferred that the dark current of the sensor on the InP substrate is generated by the threading dislocations propagating to the SL mentioned in the last section. It is expected that the suppression of threading dislocation in the SLs would lower the dark current density.

#### 4. Conclusion

Mid-infrared sensors with cutoff wavelength of 6.5  $\mu\text{m}$  have been demonstrated using InAs/GaSb SLs absorption layer grown on InP substrates for the first time. The crystalline quality of SL has been improved by using thick GaSb buffer layer because threading dislocations propagating to SL are reduced. SLs with high optical quality are successfully obtained on InP substrates. We conclude that InAs/GaSb SLs on InP substrates are promising for the back-illuminated sensors.

#### References

- (1) J. B. Rodriguez, C. Cervera, and P. Christol, "A type-II superlattice period with a modified InAs to GaSb thickness ratio for midwavelength infrared photodiode performance improvement," *Appl. Phys. Lett.*, 2010, vol. 96, no. 25, pp. 251113
- (2) H. Mohseni, E. Michel, J. Sandoen, and M. Razeghi, "Growth and characterization of InAs/GaSb photoconductors for long wavelength infrared range," *Appl. Phys. Lett.*, 1997, vol. 71, no. 10, pp. 1403-1405
- (3) S. D. Das, S. L. Tan, S. Zhang, Y. L. Goh, C. H. Tan, and J. David, "Development of LWIR photodiodes based on InAs/ GaSb Type II strained layer superlattices," *Proc. of 6th EMRS DTC Technical Conference*, 2009, pp. B7
- (4) M. Walther, J. Schmitz, R. Rehm, S. Kopta, F. Fuchs, J. Fleißner, W. Cabanskib, J. Ziegler, "Growth of InAs/GaSb short-period superlattices for high-resolution mid-wavelength infrared focal plane array detectors," *J. of Cryst. Growth*, 2005, vol. 278, pp. 156-161
- (5) H. S. Kim, E. Plis, J. B. Rodriguez, G. D. Bishop, Y. D. Sharma, L. R. Dawson, S. Krishna, J. Bundas, R. Cook, D. Burrows, R. Dennis, K. Patnaude, A. Reisinger, and M. Sundaram, "Mid-IR focal plane array based on type-II InAs/GaSb strain layer superlattice detector with nBn design," *Appl. Phys. Lett.*, 2008, vol. 92, no. 18, pp. 183502
- (6) P.-Y. Delaunay, B. M. Nguyen, D. Hoffman, M. Razeghi, "320x256 infrared focal plane array based on type II InAs/GaSb superlattice with a 12  $\mu\text{m}$  cutoff wavelength," *Proc. of SPIE*, 2007, vol. 6542, pp. 654204
- (7) B.-M. Nguyen, D. Hoffman, E. K. Huang, S. Bogdanov, P.-Y. Delaunay, M. Razeghi, and M. Z. Tidrow, "Demonstration of midinfrared type-II InAs/GaSb superlattice photodiodes grown on GaAs substrate," *Appl. Phys. Lett.*, 2009, vol. 94, no. 22, pp. 223506
- (8) J. W. Little, S. P. Svensson, W. A. Beck, A. C. Goldberg, and S. W. Kennerly, T. Hongsmatip, M. Winn, and P. Uppal, "Thin active region, type II superlattice photodiode arrays: Single-pixel and focal plane array characterization," *J. of Appl. Phys.*, 2007, vol. 101, no. 4, pp. 044514
- (9) M. Razeghi, S. A. Pour, E. K. Huang, G. Chen, A. Haddadi, and B. M. Nguyen "Type-II InAs/GaSb photodiodes and focal plane arrays aimed at high operating temperatures," *Opto-electron. Rev.*, 2011, vol. 19, no. 3, pp. 46-54
- (10) B. Brar, and D. Leonard, "Spiral growth of GaSb on (001) GaAs using molecular beam epitaxy," *Appl. Phys. Lett.*, 1995, vol. 66, no. 4, pp. 463-465

- (11) P. M. Thibado, B. R. Bennett, M. E. Twigg, B. V. Shanabrook, and L. J. Whitman, "Evolution of GaSb epitaxy on GaAs(001)-c(4x4)," *J. Vac. Sci. Technol. A*, 1996, vol. 14, no. 3, pp. 885-889
- (12) I. Vurgaftman, J. R. Meyer, and L. R. Ram-Mohan, "Band parameters for III-V compound semiconductors and their alloys," *J. of Appl. Phys.*, 2001, vol. 89, no. 11, pp. 5815-5875
- (13) W. M. Yim, and R. J. Paff, "Thermal expansion of AlN, sapphire, and silicon," *J. of Appl. Phys.*, 1974, vol. 45, no. 3, pp. 1456-1457
- (14) S. F. Yoon, H. Q. Zheng, P. H. Zhang, K. W. Hah, and G. I. Ng, "Molecular beam epitaxial growth of InP using a valved phosphorus cracker cell: optimization of electrical, optical and surface morphology characteristics," *Jpn. J. Appl. Phys.*, 1999, vol. 38, part 1, no. 2B, pp. 981-984

#### Contributors (The lead author is indicated by an asterisk (\*).)

##### K. MIURA\*

- Dr. Eng.  
Transmission Devices R&D Laboratories



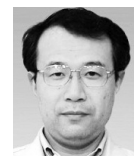
##### Y. IGUCHI

- Dr. Eng.  
Group leader, Transmission Devices  
R&D Laboratories



##### T. KATSUYAMA

- Ph. D.  
Manager, Transmission Devices R&D  
Laboratories



##### Y. KAWAMURA

- Ph. D.  
Professor, Graduate School of Engineering,  
Osaka Prefecture University

